Mechanistic Insights into Lithium-Mediated Nitrogen Reduction Reaction for Ammonia Electrosynthesis

Chengyu Zhou, and Qing Zhao*

Department of Chemical Engineering, Northeastern University, Boston, Massachusetts 02115, United States

***Corresponding Author:** Qing Zhao (E-mail: q.zhao@northeastern.edu)

Abstract

Recently, lithium-mediated nitrogen reduction reaction (Li-NRR) in nonaqueous electrolytes has proven to be an environmentally sustainable and feasible route for ammonia electrosynthesis, revealing tremendous economic and social advantages over the industrial Haber-Bosch process which consumes enormous fossil fuels and generates massive carbon dioxide emissions, and direct electrocatalytic nitrogen reduction reaction (NRR) which suffers from sluggish kinetics and poor faradaic efficiencies. However, reaction mechanisms of Li-NRR and the role of solid electrolyte interface (SEI) layer in activating N_2 remain unclear, impeding its further development. Here, using electronic structure theory, we propose a nitridation-coupled reduction mechanism and a nitrogen cycling reduction mechanism on lithium and lithium nitride surfaces, which are major components of SEI in experimental characterization. Our work reveals divergent pathways in Li-NRR from conventional direct electrocatalytic NRR, highlights the role of surface reconstruction in improving reactivity, and sheds light on enhancing efficiency of ammonia electrosynthesis.

TOC Graphic

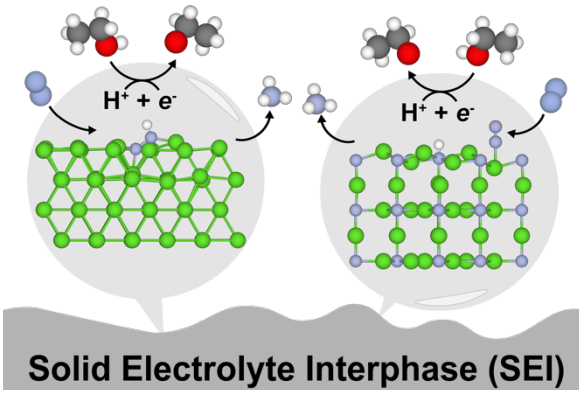

Ammonia is an important feedstock for agricultural, pharmaceutical, and chemical industries.[1] Fertilizers manufactured from ammonia have been feeding approximately 44% of the world's population over the past century.[2] In addition, ammonia is crucial to produce bioenergy and biofuels,[2] and has been recognized as a replacement for carbon-based fuels due to its large hydrogen content and high energy density. Ammonia is predominantly produced through the energy-intensive Haber–Bosch process, which reacts nitrogen and hydrogen gas at high temperatures (300–500 °C) and pressures (100–300 atm) in the presence of iron- or ruthenium-based catalysts.[3] Unfortunately, this process consumes enormous unsustainable fossil fuels and generates massive carbon dioxide emissions, and thus is not environmentally sustainable.

Tremendous efforts have been devoted to developing alternative methods for ammonia synthesis under milder or ambient conditions, including electrocatalysis, photocatalysis, enzyme catalysis, nitrogenase mimics, plasma-driven transformations, and chemical looping.[4] Among these approaches, the renewable energy-powered electrochemical synthesis offers the potential for on-site production using small-scale devices and eliminates the need for high temperatures or flammable and toxic solvents. Generally, the electrocatalytic reduction of N_2 to NH_3 can be realized through two routes: direct electrocatalytic reduction in aqueous solutions and redox-mediated electroreduction in nonaqueous electrolytes. Unfortunately, a recent paper assessed a wide range of experimental studies on ammonia electrosynthesis, including 127 direct and 16 redox-mediated nitrogen reduction reaction (NRR) routes, and concluded that nearly none of the direct electrocatalytic NRR route generates ammonia due to the competitive hydrogen evolution reaction (HER), and that the reported measurable activities erroneously result from contamination by ammonia or nitrogen-containing compounds.[5] Instead, lithium-mediated nitrogen reduction reaction (Li-NRR) in nonaqueous electrolytes has been validated to produce ammonia with reasonable reaction rates and faradaic efficiencies through rigorous experimental protocols.[6-16]

Divergent from conventional electrocatalytic NRR in which N_2 and proton sources directly react on the cathode surface, Li-NRR is catalyzed on a solid electrolyte interphase (SEI) layer formed on the cathode, composing of metallic lithium and its passivation layer derived from the nonaqueous electrolytes.[17] In addition, ethanol has been used as the proton donor to avoid HER prevalent in aqueous routes by limiting the availability of proton sources.[6-9,11,18] Recently, significant progress has been made in this area to improve efficiencies of ammonia electrosynthesis.[8,9,11-16,19-24] For example, Lazouski and Manthiram used a platinum-coated stainless steel cloth

paired with hydrogen oxidation, achieving a faradaic efficiency of 35 ± 6% with an ammonia partial current density of 8.8 ± 1.4 mA cm^{-2}.[9] Suryanto and MacFarlane demonstrated an ammonia production rate of 53 ± 1 nmol/s^1cm^2 at a faradaic efficiency of 69 ± 1% when introducing phosphonium salt as a proton shuttle.[14] Du and Simonov reported an ammonia yield rates of 150 ± 20 nmol/s^1cm^2 and a current-to-ammonia efficiency that is close to 100% by using optimal electrolytes with optimized concentration.[15] Fu and Chorkendorff designed a continuous-flow reactor coupled with hydrogen oxidation reaction on PtAu anode catalyst, achieving a faradaic efficiency of up to 61 ± 1% and an energy efficiency of 13 ± 1% for ammonia generation.[16]

Though Li-NRR represents the most promising ammonia generation technology, these redox-mediated routes usually operate at high potentials,[9,14,19,25] which increases the energy cost considerably, making the commercialization target challenging.[26] Therefore, further efforts in both fundamental understanding and systematic engineering are critical to enhance the reaction rate, selectivity, and energy efficiency. Essentially, elucidating Li-NRR reaction pathways can fill in fundamental gaps in understanding the chemistry of such process.[13,27] Though it is generally accepted that the redox mediator, Li^+, is first reduced to metallic lithium on cathode surface, and then activates N_2 via a series of proton-coupled electron transfer (PCET) steps to produce ammonia,[16-18] yet how metallic lithium catalyzes N_2 activation and reduction remains unclear. Here, to fill this fundamental gap, we performed density functional theory (DFT) calculations to understand reaction mechanisms of N_2 activation and reduction to ammonia on lithium and lithium nitride surfaces, which are characterized as major components of SEI formed on cathode using multiple experimental techniques, including X-ray photoelectron spectroscopy (XPS), X-ray diffraction (XRD), and cryogenic transmission electron microscopy (cryo-TEM).[8,9,15,16,28,29] We discovered a nitridation-coupled reduction mechanism on lithium and a nitrogen-cycling reduction mechanism on lithium nitride surface, divergent from the traditional N_2 associative and dissociative mechanisms proposed for direct electrocatalytic NRR (Figure 1).[30]

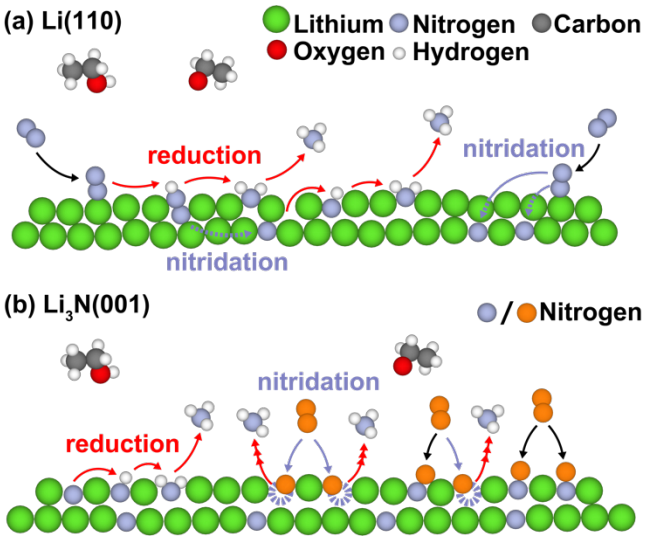

Figure 1. DFT-proposed Li-NRR pathways of (a) nitridation-coupled reduction mechanism on Li(110), and (b) nitrogen-cycling reduction mechanism on $Li_3N(001)$. Black, red, and blue arrows indicate nitrogen adsorption, reduction, and nitridation steps, respectively. Atoms are colored as follows: lithium in green, nitrogen in blue or orange, carbon in dark gray, oxygen in red, and hydrogen in light gray. Empty blue spheres on $Li_3N(001)$ indicate nitrogen vacancies created by nitrogen reduction. For clarification, nitrogen atoms are colored in either blue or orange to distinguish their original sources from $Li_3N(001)$ or N_2 in part (b).

Nitridation-coupled reduction mechanism on Li(110). We performed periodic DFT calculations with Perdew-Burke-Ernzerhof[31] exchange-correlation functional and Grimme's D3 van der Waals correction[32,33] (DFT-PBE-D3) to determine the reaction pathways and reaction energies of Li-NRR (see Supporting Information or SI Method section for computational details). To simulate the lithium surface, we used Li(110) as it is the most stable lithium facet (SI Figure S1).[34] We started from N_2 associative mechanism on Li(110), in which PCET steps happen prior to the cleavage of the N-N bond. Before optimizing the minimum energy paths, we screened all possible adsorption sites for all intermediates and used the most favorable adsorption sites in our mechanistic analysis (SI Table S1). Surprisingly, we observed that the N-N bond breaks after two successive PCET steps, forming a $*NH_2$ (adsorbed NH_2; * refers to an adsorption site) and a $^{\#}N$ (nitride; $^{\#}$ refers to a nitridation site), different from the traditional N_2 associative path, in which N-N bond cleavage is concurrent after three PCET steps with the release of the first NH_3 molecule formed (Figure 1a).

More precisely, our nitridation-coupled reduction mechanism on Li(110) reveals that N_2 is firstly adsorbed onto the surface, forming an end-on $*N_2$ with an adsorption energy of -0.33 eV

(Figure 2). Subsequently, $*N_2$ is reduced to $*N_2H$ with a reaction energy of -1.58 eV, indicating that the first PCET step is thermodynamically favorable. Afterwards, $*N_2H$ undergoes the second PCET, as well as the N-N bond cleavage, forming a $*NH_2$ adsorbed on the surface with the other N diffusing into the subsurface layer in a nitridation process (Figure 2). This N-N bond breaking step is energetically favorable with a very negative reaction energy of -2.09 eV, indicating that lithium surfaces are extremely reactive in activating N-N bond. After that, the $*NH_2$ is further reduced to form a NH_3 molecule released from the surface with a positive reaction energy of 1.33 eV, indicating that the last PCET step towards formation of NH_3 is the rate-limiting step in the overall Li-NRR pathway. In contrast, previous studies proposed that either the first or second reduction step, i.e., $*N_2 \rightarrow *N_2H$ or $*N_2H \rightarrow *N_2H_2$, is potential rate-limiting step for N_2 associative pathway on metallic surfaces.[35-38]

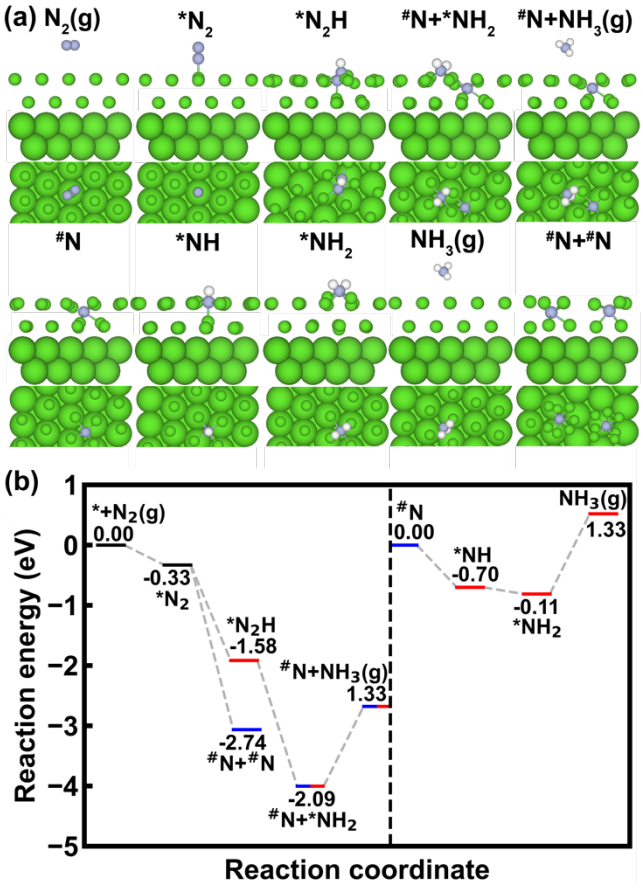

Figure 2. (a) Side (top) and top (bottom) views of structures and (b) corresponding energetics along the pathway of the proposed nitridation-coupled reduction mechanism of N_2 to NH_3 on Li(110). Atoms are colored as follows: lithium in green, nitrogen in blue, and hydrogen in light

gray. Spheres representing lithium atoms in the two topmost layers are scaled down to show the nitridated nitrogen atoms in the subsurface layer. Black, red, and blue lines in (b) indicate nitrogen adsorption, reduction, and nitridation steps, respectively.

We next studied whether the formed $^{\#}N$ in the Li(110) subsurface layer can be reduced to form a second NH_3 molecule (Figure 2). Our simulation indicates that the $^{\#}N$ can be reduced to a *NH with a reaction energy of -0.70 eV, in which the $^{\#}N$ moves from the Li(110) subsurface layer to surface layer upon protonation. *NH is then reduced to $*NH_2$ with a reaction energy of -0.11eV. Finally, $*NH_2$ is reduced to form a NH_3 molecule with a positive reaction energy of 1.33 eV, consistent with the energy required by the last PCET step of forming the first NH_3 molecule, confirming again that the protonation of $*NH_2$ is the rate-limiting step of Li-NRR.

In addition to the N_2 associative mechanism described above, we also studied the possibility of N_2 dissociative mechanism on Li(110), in which N-N bond breaking happens first before any PCET step. We observed that accompanied by the N-N cleavage, two $^{\#}N$ forms in the subsurface layer with a very favorable reaction energy of -2.74 eV (Figure 2). After that, each $^{\#}N$ proceeds through three PCET steps to form a NH_3 molecule (*vide supra*). Here, the N_2 dissociative step is simply chemical, rather than electrochemical, reaction since no electron transfer. That is to say, the energetics will not change with the applied potential, whereas PCET steps, including the first step of N_2 associative mechanism, can be affected by the applied potential and therefore potentially could be more favorable. Thus, the overall Li-NRR pathway on Li(110) could potentially involve both N_2 associative and dissociative mechanisms: $N_2 \rightarrow *N_2 \rightarrow *N_2H \rightarrow *NH_2 + {}^{\#}N \rightarrow NH_3 + {}^{\#}N$ or $N_2 \rightarrow *N_2 \rightarrow {}^{\#}N + {}^{\#}N$ and $^{\#}N \rightarrow *NH \rightarrow *NH_2 \rightarrow NH_3$. However, the nitridation-coupled reduction mechanism proposed here for Li-NRR significantly differ from those reported previously on metallic surfaces[35-38] because (1) nitridation happens along with reduction and the formed $^{\#}N$ can be reduced to NH_3 as a short-lived intermediate, (2) all steps are energetically favorable except for the last PCET step of $*NH_2$ reduction towards formation and desorption of NH_3, i.e., $*NH_2 \rightarrow NH_3$ (1.33 eV), which is believed to be the rate-limiting step, (3) N-N bond cleavage has very negative reaction energies in both dissociative and associative mechanisms, i.e., $*N_2 \rightarrow {}^{\#}N + {}^{\#}N$ (-2.74 eV) and $*N_2H \rightarrow *NH_2 + {}^{\#}N$ (-2.09 eV), (4) N-N bond breaks after two successive PCET steps in the associative mechanism, not after three PCET steps upon the formation of NH_3, (5) lithium surface reconstruction plays a vital role to accommodate nitrogen activation, reduction, and nitridation in Li-NRR.

Nitrogen-cycling reduction mechanism on $Li_3N(001)$. We next determined the reaction pathway of NRR on lithium nitride surface, which is another major inorganic component of SEI from experimental characterization,[8,15,29] at the DFT-PBE-D3 level of theory. We selected $Li_3N(001)$ surface as it is the most stable facet (SI Figure S2).[39] Divergent from the nitridation-coupled reduction mechanism on Li(110), we proposed a nitrogen-cycling reduction mechanism on $Li_3N(001)$ (Figure 1b and 3), in which reduction occurs at a lattice N site, $^{\dagger}N$ († refers to a lattice site), not at the adsorbed N_2. We predicted that $^{\dagger}N$ is first reduced to $^{\dagger}NH$ with a very negative reaction energy of -2.28 eV (Figure 3). $^{\dagger}NH$ is then reduced to $^{\dagger}NH_2$ with a favorable reaction energy of -0.79 eV, followed by the third PCET step leading to formation and desorption of NH_3 on/from the surface with a reaction energy of 1.28 eV. Consistent with the reaction mechanism on Li(110), the last PCET step towards NH_3 generation is the potential rate-limiting step on $Li_3N(001)$.

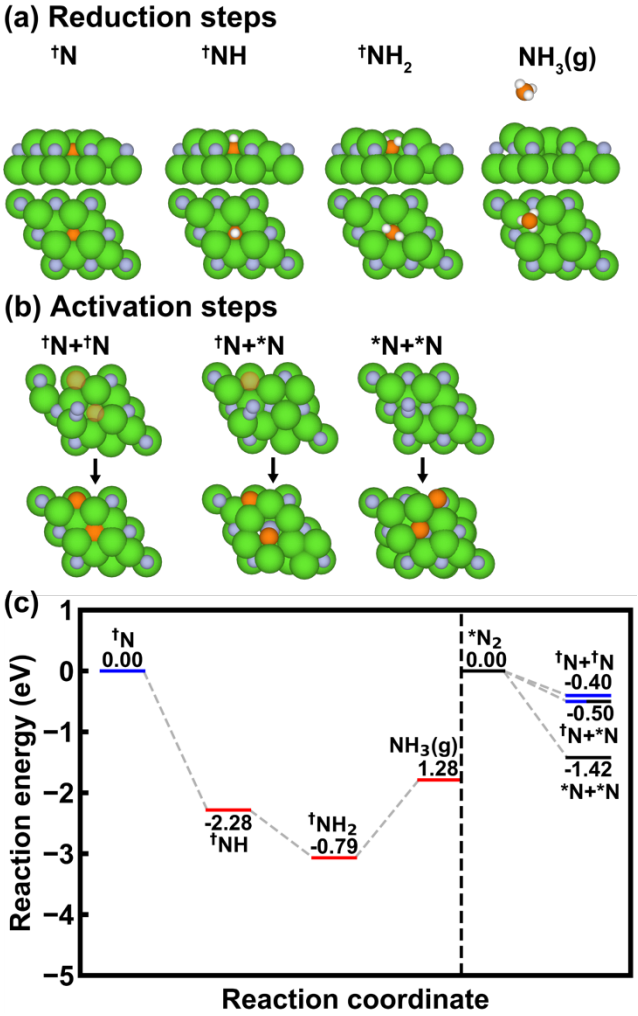

Figure 3. (a) Side (top) and top (bottom) views of structures along the reduction steps, (b) top views of structures along the activation steps, and (c) energetics of the proposed nitrogen-cycling reduction mechanism on $Li_3N(001)$. Atoms are colored as follows: lithium in green, nitrogen in blue or orange, and hydrogen in light gray. Lattice nitrogen atoms participated in the reduction reaction, as well as nitrogen atoms from N_2, are colored in orange for visualization purpose. Transparent orange spheres represent surface nitrogen vacancies. Black, red, and blue lines in (b) indicate nitrogen adsorption, reduction, and nitridation steps, respectively.

Apparently, surface nitrogen vacancies are created upon the release of the NH_3 molecule in the above lattice nitrogen participation mechanism. We next examined the possibility of N_2 activation via reversible formation of surface N vacancies. We observed three possible pathways for N_2 activation: (1) $*N_2 \rightarrow {}^{\dagger}N + {}^{\dagger}N$, in which $*N_2$ undergoes dissociative adsorption to fill two surface N vacancies, forming two ${}^{\dagger}N$ with a reaction energy of -0.40 eV, (2) $*N_2 \rightarrow {}^{\dagger}N + *N$, in which one dissociated N fills one N vacancy, while the other dissociated N adsorbs on a ${}^{\dagger}N$, forming a $*N_2$ with a reaction energy of -0.50 eV, and (3) $*N_2 \rightarrow *N + *N$, in which both dissociated N atoms adsorb on two lattice N sites (${}^{\dagger}N$) with a reaction energy of -1.42 eV (Figure 3). All N_2 activation steps are energetically favorable, and their favorability highly depends on the availabilities of N vacancy sites and thus the accessibility of proton sources to produce NH_3.

Overall, the nitrogen-cycling reduction mechanism of NRR on $Li_3N(100)$ proceeds via ${}^{\dagger}N \rightarrow {}^{\dagger}NH \rightarrow {}^{\dagger}NH_2 \rightarrow NH_3$ and $*N_2 \rightarrow {}^{\dagger}N + {}^{\dagger}N$ or $*N_2 \rightarrow {}^{\dagger}N + *N$ or $*N_2 \rightarrow *N + *N$, in which reversible formation of surface N vacancies is critical for nitrogen reduction towards NH_3 generation. Similar to the energetics on Li(110), all steps are favorable except for the last PCET step of ${}^{\dagger}NH_2 \rightarrow NH_3$, which is believed to be the rate-limiting step with a positive reaction energy of 1.28 eV. It is noteworthy that we observed significant surface reconstructions throughout the entire reaction pathway due to the formation of surface N vacancies sites, which provide active sites for nitrogen activation and reduction and thus are crucial to the overall catalytic performance.

In addition to thermodynamic analysis, kinetics modeling is essential for a more comprehensive understanding of the proposed nitridation-coupled reduction mechanism on lithium surface and the nitrogen-cycling reduction mechanism on lithium nitride surface. Here, we highlight that due to significant surface reconstructions, it is extremely challenging to locate the transition states and thus determine the energy barriers using conventional methodologies, such as climbing-image nudged elastic band (CI-NEB) method.[40,41] Specifically, the challenge is to simulate the realistic electrochemical condition of Li-NRR, including the amorphous and

dynamically evolved SEI layer, the applied potentials, the nonaqueous electrolytes, and surface reconstructions. Recently, Ludwig and Nørskov successfully obtained the reaction barrier of N_2 dissociation on lithium surface using a combination of DFT-based metadynamics and CI-NEB.[42] Following this success, we are currently simulating reaction barriers of the full Li-NRR mechanisms on both lithium and lithium nitride surfaces using metadynamics and benchmarking different explicit solvation models to consider the effects of electrolytes. Ultimately, this will allow us to complete the full mechanistic picture of lithium-mediated ammonia electrosynthesis.

In summary, we applied electronic structure theory to determine the reaction mechanisms of Li-NRR on two representative surfaces, lithium and lithium nitride, as major inorganic components of SEI. We find a new nitridation-coupled reduction mechanism on lithium surface in which nitridation plays an important role for nitrogen activation, as well as a new nitrogen-cycling reduction mechanism on lithium nitride surface in which nitrogen lattice participation via reversible formation of surface nitrogen vacancies is critical. We demonstrate that the Li-NRR mechanisms switch from the generally proposed nitrogen associative and dissociative mechanisms on metallic surfaces to these new ones with significant surface reconstructions. This provides new fundamental understanding into the design of catalysts for ammonia electrosynthesis.

Corresponding Author

q.zhao@northeastern.edu

Supporting Information

Computational details; geometries for Li(110) and Li_3N(001) surface periodic slab models; stabilities for different adsorption sites of all intermediates. (PDF)

VASP structure files for the slab models are provided as a compressed zip file. (ZIP)

Notes

The authors declare no competing financial interest.

Acknowledgments

The authors acknowledge support by the National Science Foundation under Award No. 2349619 and by Northeastern University, Chemical Engineering Department under start-up funding. This

work was carried out using computational resources from Discovery, Research Computing at Northeastern University.

References

1. Yusov, M. A.; Manthiram, K. Beyond Lithium for Sustainable Ammonia Synthesis. *Nat. Mater.* **2024**, *23* (1), 31-32.
2. Erisman, J. W.; Sutton, M. A.; Galloway, J.; Klimont, Z.; Winiwarter, W. How a Century of Ammonia Synthesis Changed the World. *Nat. Geosci.* **2008**, *1*, 636-639.
3. Smith, C.; Hill, A. K.; Torrente-Murciano, L. Current and Future Role of Haber–Bosch Ammonia in a Carbon-Free Energy Landscape. *Energy Environ. Sci.* **2020**, *13* (2), 331-344.
4. Chen, J. G.; Crooks, R. M.; Seefeldt, L. C.; Bren, K. L.; Bullock, R. M.; Darensbourg, M. Y.; Holland, P. L.; Hoffman, B.; Janik, M. J.; Jones, A. K.; Kanatzidis, M. G.; King, P.; Lancaster, K. M.; Lymar, S. V.; Pfromm, P.; Schneider, W. F.; Schrock, R. R. Beyond Fossil Fuel-Driven Nitrogen Transformations. *Science* **2018**, *360* (6391).
5. Choi, J.; Suryanto, B. H. R.; Wang, D.; Du, H. L.; Hodgetts, R. Y.; Ferrero Vallana, F. M.; MacFarlane, D. R.; Simonov, A. N. Identification and Elimination of False Positives in Electrochemical Nitrogen Reduction Studies. *Nat. Commun.* **2020**, *11* (1), 5546.
6. Tsuneto, A.; Kudo, A.; Sakata, T. Efficient Electrochemical Reduction of N_2 to NH_3 Catalyzed by Lithium. *Chem. Lett.* **1993**, *22* (5), 851-854.
7. Tsuneto, A.; Kudo, A.; Sakata, T. Lithium-Mediated Electrochemical Reduction of High Pressure N_2 to NH_3. *J. Electroanal. Chem.* **1994**, *367* (1-2), 183-188.
8. Lazouski, N.; Schiffer, Z. J.; Williams, K.; Manthiram, K. Understanding Continuous Lithium-Mediated Electrochemical Nitrogen Reduction. *Joule* **2019**, *3* (4), 1127-1139.
9. Lazouski, N.; Chung, M.; Williams, K.; Gala, M. L.; Manthiram, K. Non-Aqueous Gas Diffusion Electrodes for Rapid Ammonia Synthesis from Nitrogen and Water-Splitting-Derived Hydrogen. *Nat. Catal.* **2020**, *3* (5), 463-469.
10. Lazouski, N.; Steinberg, K. J.; Gala, M. L.; Krishnamurthy, D.; Viswanathan, V.; Manthiram, K. Proton Donors Induce a Differential Transport Effect for Selectivity toward Ammonia in Lithium-Mediated Nitrogen Reduction. *ACS Catal.* **2022**, *12* (9), 5197-5208.
11. Andersen, S. Z.; Colic, V.; Yang, S.; Schwalbe, J. A.; Nielander, A. C.; McEnaney, J. M.; Enemark-Rasmussen, K.; Baker, J. G.; Singh, A. R.; Rohr, B. A.; Statt, M. J.; Blair, S. J.; Mezzavilla, S.; Kibsgaard, J.; Vesborg, P. C. K.; Cargnello, M.; Bent, S. F.; Jaramillo, T. F.; Stephens, I. E. L.; Nørskov, J. K.; Chorkendorff, I. A Rigorous Electrochemical Ammonia Synthesis Protocol with Quantitative Isotope Measurements. *Nature* **2019**, *570* (7762), 504-508.
12. Andersen, S. Z.; Statt, M. J.; Bukas, V. J.; Shapel, S. G.; Pedersen, J. B.; Krempl, K.; Saccoccio, M.; Chakraborty, D.; Kibsgaard, J.; Vesborg, P. C. K.; Nørskov, J.; Chorkendorff, I. Increasing Stability, Efficiency, and Fundamental Understanding of Lithium-Mediated Electrochemical Nitrogen Reduction. *Energy Environ. Sci.* **2020**, *13* (11), 4291-4300.
13. Cai, X.; Fu, C.; Iriawan, H.; Yang, F.; Wu, A.; Luo, L.; Shen, S.; Wei, G.; Shao-Horn, Y.; Zhang, J. Lithium-Mediated Electrochemical Nitrogen Reduction: Mechanistic Insights to Enhance Performance. *iScience* **2021**, *24* (10), 103105.

14. Suryanto, B. H. R., ; Matuszek, K.; Choi, J.; Hodgetts, R. Y.; Du, H.-L.; Bakker, J. M.; Kang, C. S. M.; Cherepanov, P. V.; Simonov, A. N.; MacFarlane, D. R. Nitrogen Reduction to Ammonia at High Efficiency and Rates Based on a Phosphonium Proton Shuttle. *Science* **2021**, *372* (6547), 1187-1191.
15. Du, H. L.; Chatti, M.; Hodgetts, R. Y.; Cherepanov, P. V.; Nguyen, C. K.; Matuszek, K.; MacFarlane, D. R.; Simonov, A. N. Electroreduction of Nitrogen with Almost 100% Current-to-Ammonia Efficiency. *Nature* **2022**, *609* (7928), 722-727.
16. Fu, X. B.; Pedersen, J. B.; Zhou, Y. Y.; Saccoccio, M.; Li, S. F.; Salinas, R.; Li, K. T.; Andersen, S. Z.; Xu, A. N.; Deissler, N. H.; Mygind, J. B. V.; Wei, C.; Kibsgaard, J.; Vesborg, P. C. K.; Nørskov, J. K.; Chorkendorff, I. Continuous-Flow Electrosynthesis of Ammonia by Nitrogen Reduction and Hydrogen Oxidation. *Science* **2023**, *379* (6633), 707-712.
17. Chang, W.; Jain, A.; Rezaie, F.; Manthiram, K. Lithium-Mediated Nitrogen Reduction to Ammonia via the Catalytic Solid–Electrolyte Interphase. *Nat. Catal.* **2024**, *7* (3), 231-241.
18. Schwalbe, J. A.; Statt, M. J.; Chosy, C.; Singh, A. R.; Rohr, B. A.; Nielander, A. C.; Andersen, S. Z.; McEnaney, J. M.; Baker, J. G.; Jaramillo, T. F.; Nørskov, J. K.; Cargnello, M. A Combined Theory-Experiment Analysis of the Surface Species in Lithium-Mediated NH_3 Electrosynthesis. *ChemElectroChem* **2020**, *7* (7), 1542-1549.
19. McEnaney, J. M.; Singh, A. R.; Schwalbe, J. A.; Kibsgaard, J.; Lin, J. C.; Cargnello, M.; Jaramillo, T. F.; Nørskov, J. K. Ammonia Synthesis from N_2 and H_2O Using a Lithium Cycling Electrification Strategy at Atmospheric Pressure. *Energy Environ. Sci.* **2017**, *10* (7), 1621-1630.
20. Li, K.; Andersen, S. Z.; Statt, M. J.; Saccoccio, M.; Bukas, V. J.; Krempl, K.; Sažinas, R.; Pedersen, J. B.; Shadravan, V.; Zhou, Y.; Chakraborty, D.; Kibsgaard, J.; Vesborg, P. C. K.; Nørskov, J. K.; Chorkendorff, I. Enhancement of Lithium-Mediated Ammonia Synthesis by Addition of Oxygen. *Science* **2021**, *374* (6575), 1593-1597.
21. Li, K.; Shapel, S. G.; Hochfilzer, D.; Pedersen, J. B.; Krempl, K.; Andersen, S. Z.; Sažinas, R.; Saccoccio, M.; Li, S.; Chakraborty, D.; Kibsgaard, J.; Vesborg, P. C. K.; Nørskov, J. K.; Chorkendorff, I. Increasing Current Density of Li-Mediated Ammonia Synthesis with High Surface Area Copper Electrodes. *ACS Energy Lett.* **2021**, *7* (1), 36-41.
22. Li, S.; Zhou, Y.; Li, K.; Saccoccio, M.; Sazinas, R.; Andersen, S. Z.; Pedersen, J. B.; Fu, X.; Shadravan, V.; Chakraborty, D.; Kibsgaard, J.; Vesborg, P. C. K.; Nørskov, J. K.; Chorkendorff, I. Electrosynthesis of Ammonia with High Selectivity and High Rates via Engineering of the Solid-Electrolyte Interphase. *Joule* **2022**, *6* (9), 2083-2101.
23. Fu, X.; Niemann, V. A.; Zhou, Y.; Li, S.; Zhang, K.; Pedersen, J. B.; Saccoccio, M.; Andersen, S. Z.; Enemark-Rasmussen, K.; Benedek, P.; Xu, A.; Deissler, N. H.; Mygind, J. B. V.; Nielander, A. C.; Kibsgaard, J.; Vesborg, P. C. K.; Nørskov, J. K.; Jaramillo, T. F.; Chorkendorff, I. Calcium-Mediated Nitrogen Reduction for Electrochemical Ammonia Synthesis. *Nat. Mater.* **2024**, *23* (1), 101-107.
24. Iriawan, H.; Herzog, A.; Yu, S.; Ceribelli, N.; Shao-Horn, Y. Upshifting Lithium Plating Potential To Enhance Electrochemical Lithium Mediated Ammonia Synthesis. *ACS Energy Lett.* **2024**, 4883-4891.
25. Westhead, O.; Tort, R.; Spry, M.; Rietbrock, J.; Jervis, R.; Grimaud, A.; Bagger, A.; Stephens, I. E. L. The Origin of Overpotential in Lithium-Mediated Nitrogen Reduction. *Faraday Discuss* **2023**, *243* (0), 321-338.
26. Lazouski, N.; Limaye, A.; Bose, A.; Gala, M. L.; Manthiram, K.; Mallapragada, D. S. Cost and Performance Targets for Fully Electrochemical Ammonia Production under Flexible Operation. *ACS Energy Lett.* **2022**, *7* (8), 2627-2633.

27. Fu, X.; Zhang, J.; Kang, Y. Recent Advances and Challenges of Electrochemical Ammonia Synthesis. *Chem Catal.* **2022**, *2* (10), 2590-2613.
28. Fu, X.; Li, S.; Deissler, N. H.; Mygind, J. B. V.; Kibsgaard, J.; Chorkendorff, I. Effect of Lithium Salt on Lithium-Mediated Ammonia Synthesis. *ACS Energy Lett.* **2024**, *9* (8), 3790-3795.
29. Steinberg, K.; Yuan, X.; Klein, C. K.; Lazouski, N.; Mecklenburg, M.; Manthiram, K.; Li, Y. Imaging of Nitrogen Fixation at Lithium Solid Electrolyte Interphases via Cryo-Electron Microscopy. *Nat. Energy* **2022**, *8* (2), 138-148.
30. Cui, X.; Tang, C.; Zhang, Q. A Review of Electrocatalytic Reduction of Dinitrogen to Ammonia under Ambient Conditions. *Adv. Energy Mater.* **2018**, *8* (22), 1800369.
31. Perdew, J. P.; Burke, K.; Ernzerhof, M. Generalized Gradient Approximation Made Simple. *Phys. Rev. Lett.* **1996**, *77*, 3865-3868.
32. Grimme, S.; Antony, J.; Ehrlich, S.; Krieg, H. A Consistent and Accurate Ab Initio Parametrization of Density Functional Dispersion Correction (DFT-D) for the 94 Elements H-Pu. *J. Chem. Phys.* **2010**, *132* (15), 154104.
33. Grimme, S.; Ehrlich, S.; Goerigk, L. Effect of the Damping Function in Dispersion Corrected Density Functional Theory. *J. Comput. Chem.* **2011**, *32* (7), 1456-1465.
34. Hagopian, A.; Doublet, M.-L.; Filhol, J.-S. Thermodynamic Origin of Dendrite Growth in Metal Anode Batteries. *Energy Environ. Sci.* **2020**, *13* (12), 5186-5197.
35. Dahl, S.; Logadottir, A.; Egeberg, R. C.; Larsen, J. H.; Chorkendorff, I.; Törnqvist, E.; Nørskov, J. K. Role of Steps in N_2 Activation on Ru(0001). *Phys. Rev. Lett.* **1999**, *83*, 1814-1817.
36. Rod, T. H.; Logadottir, A.; Nørskov, J. K. Ammonia synthesis at low temperatures. *J. Chem. Phys.* **2000**, *112* (12), 5343-5347.
37. Logadóttir, Á.; Nørskov, J. K. Ammonia Synthesis over a Ru(0001) Surface Studied by Density Functional Calculations. *J. Catal.* **2003**, *220* (2), 273-279.
38. Skúlason, E.; Bligaard, T.; Gudmundsdottir, S.; Studt, F.; Rossmeisl, J.; Abild-Pedersen, F.; Vegge, T.; Jonsson, H.; Nørskov, J. K. A Theoretical Evaluation of Possible Transition Metal Electro-Catalysts for N_2 Reduction. *Phys. Chem. Chem. Phys.* **2012**, *14* (3), 1235-1245.
39. Jin, H.M.; Luo, J.Z.; Wu, P. Adsorption and Dissociation of Hydrogen on Surface: A First Principles Study. *Appl. Phys. Lett.* **2007**, *90*, 084101.
40. Henkelman, G.; Uberuaga, B. P.; Jónsson, H. A Climbing Image Nudged Elastic Band Method for Finding Saddle Points and Minimum Energy Paths. *J. Chem. Phys.* **2000**, *113* (22), 9901-9904.
41. Henkelman, G.; Jónsson, H. Improved Tangent Estimate in the Nudged Elastic Band Method for Finding Minimum Energy Paths and Saddle Points. *J. Chem. Phys.* **2000**, *113* (22), 9978-9985.
42. Ludwig, T.; Singh, A. R.; Nørskov, J. K. Subsurface Nitrogen Dissociation Kinetics in Lithium Metal from Metadynamics. *J. Phys. Chem. C* **2020**, *124* (48), 26368-26378.